

Optical Beam Jitter Control

R. Joseph Watkins*, Hong-Jen Chen, Brij N. Agrawal, Young. S. Shin
Department of Mechanical and Astronautical Engineering, Naval Postgraduate School,
Monterey, CA, USA 93943

Keywords: Pointing, Laser Communication, Jitter Rejection, Fast Steering Mirrors

ABSTRACT

For several future imaging and communications spacecraft, a challenging area of technology development is the fine acquisition, tracking, and pointing (ATP) control of the spacecraft and its payload. For example, some spacecraft with large aperture(s) in the range of 10~30 m diameter requires a few arc-seconds accuracy, 10~15 nano-radians jitter, and a fast slewing rate to acquire the target. Furthermore these stringent requirements are at risk of great structure and control interactions. This paper we will focus on the control of optical beam jitter. A Laser Jitter Control (LJC) testbed has been constructed to test jitter algorithms. The testbed consists of two fast steering mirrors (FSM), three position sensing modules (PSM), one diode laser, and several beam splitters and mirrors, all on an isolated Newport optical bench. Jitter is injected with one FSM and the other FSM is used to control it. The jitter spectrum, representing the on-orbit spacecraft and beam jitter environment, contains not only narrow band noise due to rotating devices such as gyroscopes and reaction wheels but also broadband noise. The performance of a Wiener Filter - adaptive algorithm with ideal reference signal is established as the baseline for comparison of adaptive control methods in suppressing both broadband and narrowband disturbances. Specifically, the Least Mean Squares (LMS) approach and the Gradient Adaptive Lattice (GAL) approach are investigated during these experiments.

1. INTRODUCTION

The ability to accurately point a laser beam is becoming increasingly important. The use of satellites to relay laser communications through space and from/to earth could increase available bandwidth and thus data transfer rate by several orders of magnitude. The use of lasers as defensive weapons, especially against missile systems, will require extremely accurate pointing capabilities. Jitter, the undesired fluctuations in the pointing of a laser beam due to environment or structural interactions, reduces the intensity of the beam at the target, whether the beam is used as a communications system or a weapon. For example, a 100 mm diameter beam with 1 μ rad of jitter will result in roughly a 100 fold decrease in the intensity of the beam at 500 km, due to the jitter alone.

This paper summarizes the development of the Optical Relay Mirror Lab – Laser Jitter Control (LJC) Testbed, which is located in the Spacecraft Research and Design Laboratory at Naval Postgraduate School. This paper will review the progress of the research thus far. During this first phase of the research, classical control techniques are implemented to learn how the system behaves from a classical viewpoint. Next, proven adaptive means are implemented and compared to the ideal Wiener Filter, as well as to each other and the classical control model.

2. EXPERIMENTAL PLATFORM AND MATHEMATICAL MODEL

2.1. Experimental platform – Laser Jitter Control (LJC) Testbed

The LJC Testbed is constructed around two FSMs and three PSMs. A block diagram showing the arrangement is provided in Figure 1. The laser source is a 2.5 mW, 670nm diode laser. Disturbance injection is accomplished by a FSM, purchased from Baker Adaptive Optics¹, denoted as the DFSM. The Receive FSM (RFSM) was purchased from Newport Corporation². The function of these two mirrors may be easily exchanged. The experimentally determined control bandwidth of the mirrors was found using spectrum analysis to be approximately 800 Hz for the Newport mirror in both axes and about 4 kHz for the Baker mirror in both axes. The Newport mirror provides a voltage output proportional to the position of the mirror, however, the Baker mirror does not.

* rjwatkin@nps.navy.mil; phone: 1-831-656-1146; fax:1-831-656-2313; <http://www.aa.nps.navy.mil/~agrawal/srdoc/>

The computer control system is based on MATLAB release 13 and the xPC Targetbox, all from the Mathworks³. The xPC Targetbox has the ability to accept 16 differential inputs and provide 4 analog outputs. The main computer for control implementation and experiment supervision is a 2.4 GHz Dell with 1 Gbyte of RAM.

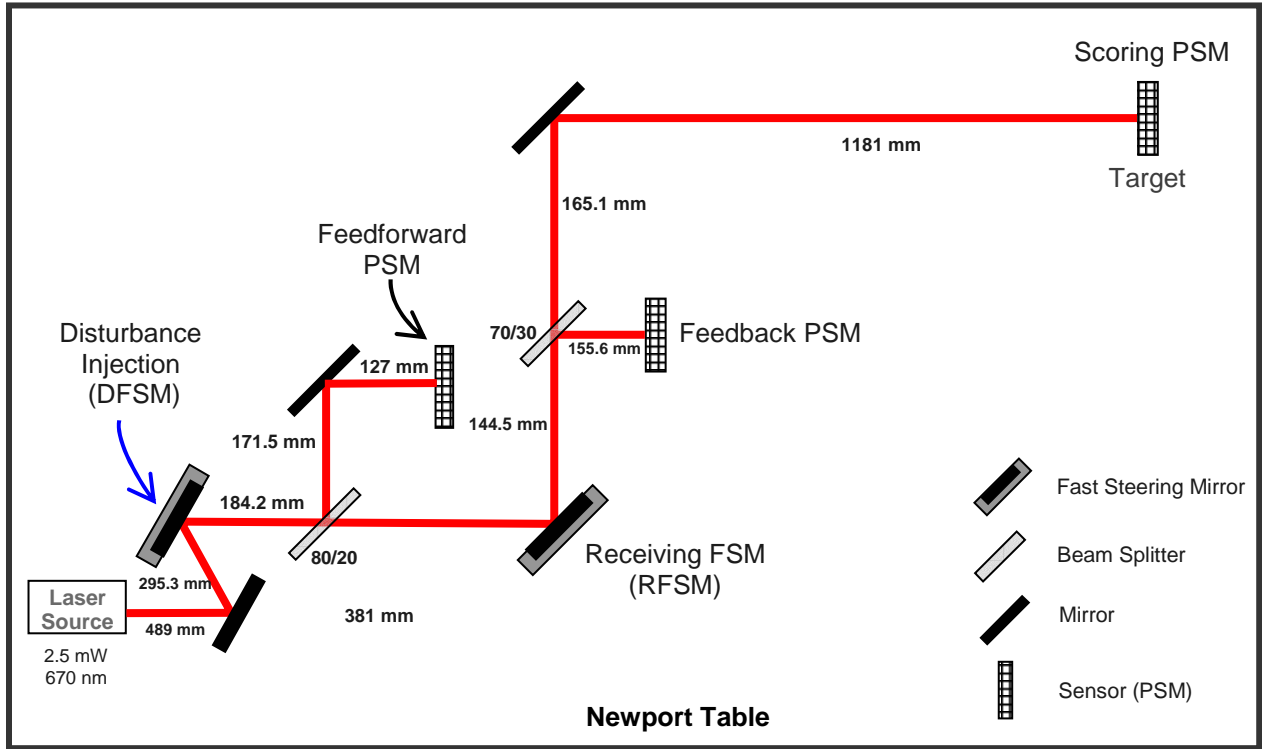


Figure 1. Laser Jitter Control Testbed

The sensors, known as Position Sensing Modules or PSM, were purchased from OnTrak Photonics Inc⁴. and have a detection area of 10mm x 10mm. Each Position Sensing Module (PSM) requires an amplifier, the OT-301. Various beam splitters and folding mirrors are used to direct the beam as desired. The detectors have a minimum sensitivity of 50-100 μ W, which drives the selection of the beam splitters and the determination of laser power. The optimum beam size for accurate detection on the PSM is between 1 and 3 mm, and the maximum allowed intensity should be less than 300 W/cm². The output range of the PSM/OT-301 detector is plus or minus 10 V and the OT-301 amplifier has a minimum noise level of 1 mV. The minimum resolution of the PSM with the OT 301 amplifier is therefore 0.5 μ m.

2.2. Mathematical model

In order to understand the setup in classical control terms, and thereby gain insight into the system, a mathematical model is constructed and control of the system using a Linear Quadratic Optimal Regulator (LQR) is first attempted. A simple second order transfer function of the Newport mirror about one axis is defined:

$$H_m(s) = \frac{\omega_n^2}{s^2 + 2\zeta\omega_n s + \omega_n^2} \quad (1)$$

where $\omega_n=5000$ rad/s (the experimentally determined value for the natural frequency of the Newport mirror) and $\zeta=0.50$. The damping ratio, ζ , was determined by comparing the model's frequency response to the actual frequency response of the mirror, and adjusting ζ accordingly.

A delay was added to account for the time lag in the command circuitry to the mirror and the detection circuitry of the PSM/OT-301:

$$H_d(s) = \frac{1}{Ts + 1} \quad (2)$$

where T is roughly 0.00024 sec. The value for T was determined by comparing the step response of the experimental system to a simulated step response using the mathematical model, and adjusting T until the simulated and actual step responses matched

The resulting State-Space set of equations for one axis is given:

$$\begin{bmatrix} \dot{V}_p \\ \dot{\theta} \\ \ddot{\theta} \end{bmatrix} = \begin{bmatrix} -1/T & 2GpDm/T & 0 \\ 0 & 0 & 1 \\ 0 & -\omega_n^2 & -2\zeta\omega_n \end{bmatrix} \begin{bmatrix} V_p \\ \theta \\ \dot{\theta} \end{bmatrix} + \begin{bmatrix} 0 \\ 0 \\ \omega_n^2 Gm \end{bmatrix} V_m + \begin{bmatrix} -GpDb/T \\ 0 \\ 0 \end{bmatrix} \theta_d \quad (3)$$

In equation (3), V_p is the voltage at the PSM, Gp is the PSM gain, V/m, and Dm is the distance from the control mirror to the PSM, m. θ is the rotation about the control mirror's x axis, Gm is the control mirror gain, rad/V, and V_m is the voltage input to the control mirror. Db is the distance from the disturbance source to the detector and θ_d is the rotation about the laser beam's x or y axis at the disturbance source. θ_d is a pseudo-random variable, considered to be band-limited white noise plus any narrow-band disturbances.

3. CONTROL ALGORITHMS

In the sections below we summarize the control and signal processing algorithms we have implemented and tested for jitter rejection on the LJC testbed, including linear quadratic regulator (LQR) control, adaptive least mean squares (LMS) algorithm and gradient adaptive lattice algorithm. In this first attempt at controlling the FSM to compensate for broad-band and narrow-band disturbances, a single-input/single-output (SISO) system is employed with each axis of the disturbance and control mirror treated separately. As the research progresses, multiple-input/multiple-output (MIMO) systems will be utilized to investigate the ability to compensate for noise using MIMO control techniques. In developing these algorithms, care must be taken to solve for the discrete solution using the sample time of the computer control system, typically 0.0005 sec.

3.1. Linear Quadratic Regulator (LQR) Control

The LQR is first developed to investigate how classical control algorithms handle broadband disturbances. Using the State-Space system of equation (3), the optimal gains are determined using the algorithms available in MATLAB. The LQR requires full state feedback, which is not available for this system: the voltage from the detector and the position of the mirror can be measured, but not the velocity of the mirror. An observer, after the method of Friedland⁵ was constructed to estimate the velocity of the mirror. The velocity may also be estimated by taking the derivative of the position, and after filtering, a usable signal was obtained using this method. Using either method resulted in satisfactory performance. The linear-quadratic optimal gains (K) were calculated to minimize the quadratic cost function

$$J = \int_0^{\infty} (x^T Q x + u^T R u) dt \quad \text{with } x \text{ being the state vector, and } u \text{ the input. The matrices } Q \text{ and } R \text{ are used to weight the}$$

relative importance of each state and the input. The control law is $u = -Kx$. The state-space system defined in Sect. 2.2 is used to solve for the optimal gains for the LQR, with increased weighting on the voltage at the detector, V_p .

3.2. Adaptive Control

In adaptive control, we adjust the *tap gains* based on the response of the system to (1) the error, (2) a reference signal correlated with the disturbance, and (3) the control input. The algorithm may use (one of) various means, such as Least Squares or other stochastic methods, to find the optimum system. In particular, the algorithm relies on *predicting* its next input, which is simply the disturbance in the case of laser jitter control, to optimize the *tap gains*. The error - the difference between the predicted signal and the system output - is then used to recalculate the gains that minimize the error in return. For the LJC Testbed, the feed-back detector is used to provide the error signal, and the feed-forward detector provides the correlated disturbance input signal. This type of control algorithm not only calculates the necessary gains, but also identifies the system, removing the requirement to mathematically model the system. The type of adaptive control used in the experimental setup utilizes predictors. One type of *forward* predictor is the transversal or ladder filter, as shown in Figure 2. One may also conduct *backward prediction*, i.e. calculate what an input was in the past, given the n current and past inputs. Both the Least Mean Squares and Gradient Adaptive Lattice filters described in Sect. 3.3 and 3.4 below were modeled after *Haykin* in Ref. 6.

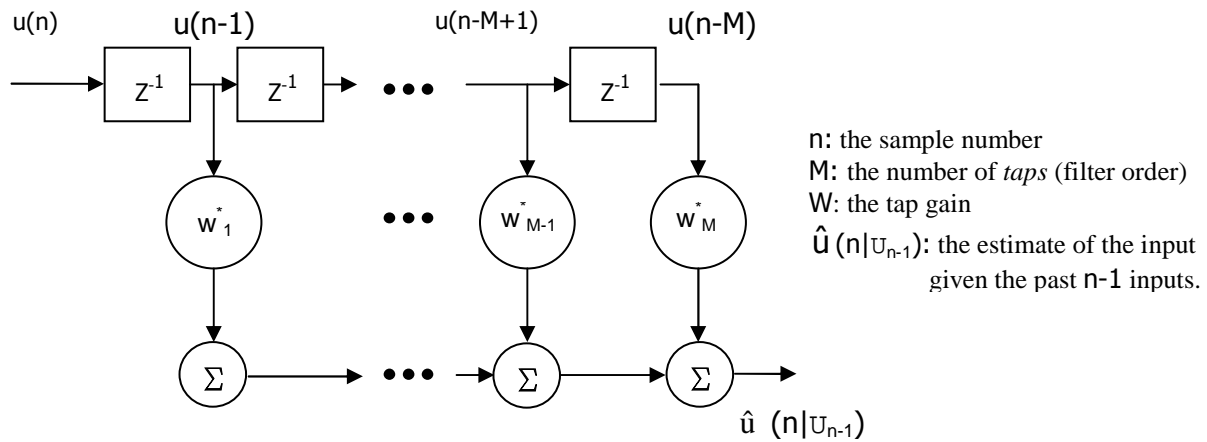


Figure 2 Transversal or ladder filter

3.2.1. Wiener filter

Using the Wiener-Hopf equations⁶, we may determine the optimum tap gains w , for the filter shown in Figure 3, given the order of the filter, the inputs and the desired output. The optimum tap gain vector is then given by $w_f = R^{-1}p$, with R defined as the correlation matrix of delayed inputs and p the cross-correlation between delayed inputs and desired output. The output of this filter should give the best possible reduction in the amplitude of the disturbance.

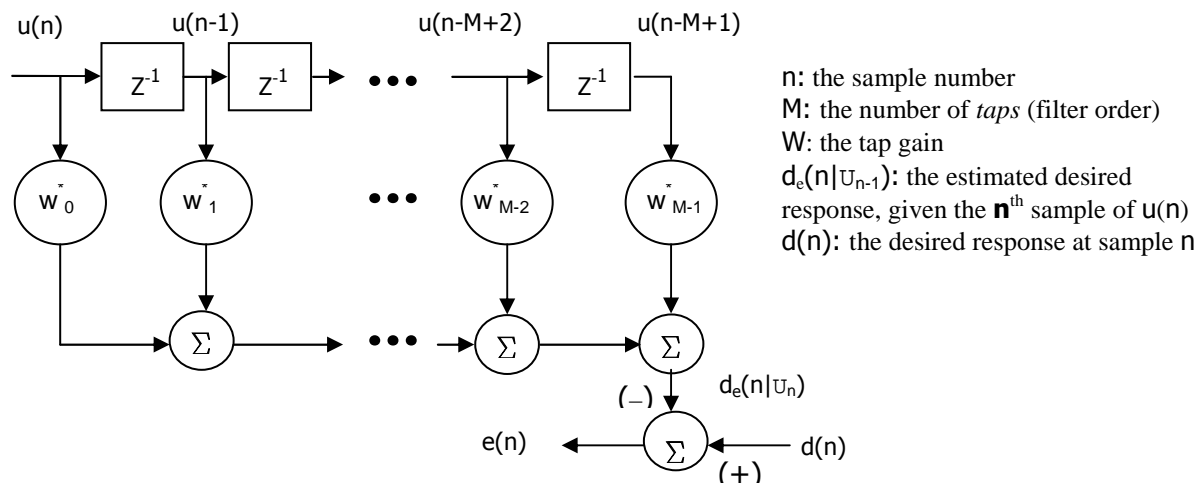


Figure 3. Compensation Scheme using the Ladder Filter

3.3. Adaptive least mean squares (LMS) algorithm

The LMS algorithm seeks to minimize or even cancel the effect of disturbance at the feedback PSM on LJC testbed using the control mirror position. The tap gain vector, \mathbf{W}_f (Figure 3) is computed using the error from the feedback PSM, vector of delayed disturbance inputs and an adaptation rate. The maximum adaptation rate, μ that can be used and maintain stability is $\mu \leq \lambda_{\max}^{-1}$ where λ_{\max} is the largest eigenvalue of the input correlation matrix^{6,7}. The adaptation rate is determined experimentally to be the value that gave the overall best reduction in the amplitude of the disturbance. The algorithm used in this experiment is similar to that given in Ref. 7, 8 and 9, but no filtering on the disturbance correlated signal is performed due to the near unity characteristic of the system transfer function within the control bandwidth.

3.4. Gradient adaptive lattice (GAL) algorithm

The GAL algorithm uses both forward and backward prediction to develop the estimate of the desired cancellation signal, which again drives the control mirror to cancel the effect of disturbance input. The construction of the GAL filter is different than the linear transversal filter in that it uses reflection coefficients vice tap gains due to the nature of the *lattice-like* structure as shown in Figure 4:

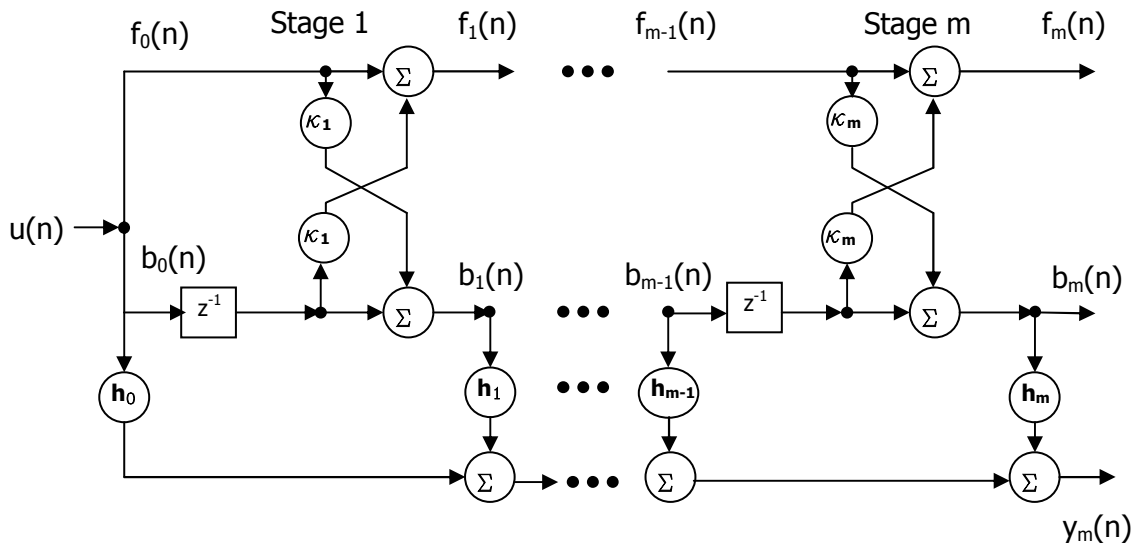


Figure 4. Lattice Filter

The forward prediction error for the i^{th} stage is given the symbol $f_i(n)$. The backward prediction error, b_i is given likewise. κ is the reflection coefficient for the i^{th} stage and h_i provides the gains to construct the desired response, y_m . The h_i are calculated using the method of least squares, with the b_i as the regressor and the h_i as the parameters to be solved. The lattice filter results in a highly efficient structure in that it is modular. Each stage only requires the output of the previous stage, and an increase in the order of the filter only requires adding additional stages⁶. Ref. 10 and 11 discuss active noise cancellation techniques using algorithms that employ the lattice filter. The same concept was used in this study, but the algorithm from Ref. 6 was used due to its simpler implementation.

4. EXPERIMENTAL RESULTS

As the jitter spectrum of optical subsystems on spacecraft on orbit contains not only narrow band noise due to rotating devices such as gyroscopes and reaction wheels but also broadband random noise, colored noise was used in our experiments to investigate the effectiveness of the control algorithms. The injected disturbance was 200 Hz band-limited white noise with two narrowband frequencies added in – one at 50 Hz and the second at 100 Hz. Both narrowband disturbance amplitudes were selected to be 25 microns at the feedback detector, placing it on the same order of magnitude as the broadband disturbance. The narrow band disturbances about each axis were also displaced in phase from each other. For the experimental setup given here, 100 μm at the feedforward detector corresponds to about a 150 μrad rotation of the laser beam axis at the disturbance mirror. Both control mirror axis were controlled

independently at the same time, with each axis treated as a SISO system. Note that a rotation of the control mirror about the x-axis of the mirror results in a y-axis displacement at the feedback detector, and vice-versa. The standard deviation of the input disturbance at the feedforward detector and the output at the feedback detector were used as a measure of performance. The feed-back detector provides the error signal and the feed-forward detector provides the input. In each of the Adaptive LMS and GAL runs, the experiment was run for a minimum of 30 seconds, which was more than enough time to allow the gains to reach their steady-state values. The responses shown in the following figures are those for the experimentally determined optimum number of stages.

In the following four sections, the performance of the control algorithms is first presented. From Figure 5 to Figure 8, the left-hand figure is the time domain results, and the right-hand figure is their corresponding Power Spectral Density (PSD). The abscissa on the time domain graph indicates the position of the centroid of the laser beam with respect to the center of the PSM, along each axis of the PSM. The input jitter is the beams position at the feedforward detector. The controlled beam is the position of the laser beam on the feedback detector. A one second period of data is shown. The PSD is only given for the x-axis, as each controller generated very similar frequency responses for each axis. A comparison of the performance of different control methods is given in Section 4.5 and the procedure in determining the optimal stage number for the adaptive algorithms is given in Section 4.6.

4.1. LQR control response

The LQR controller parameters were obtained using the State-Space model in Equation. 3 and initially using MATLAB to discretize the system and solve for the LQ-optimal gains. The sample time was 0.0005 seconds. The weighting matrix Q was constructed to give the state corresponding to the voltage at the feedback detector a weight of 1000 compared to 1 for the other two states. The input voltage to the control mirror was given a weight of 0.1 in the weighting matrix R. This resulted in a set of gains for each state, but the values were not optimum as evidenced by further experimentation. It is believed the difficulty in obtaining optimum gains using this method is due to the extremely stiff set of matrices used to model the system. Starting with these values and then using a trial an error approach, a set of gains were obtained that appear to be near the optimum in these experiments.

The LQR controller centered the beam on the feedback detector and reduced the amplitude of the input jitter by about 70 percent. The PSD shows the typical waterbed effect, with energy being added by the control system at frequencies above the control bandwidth, 200 Hz. It is apparent that the working of LQR controller does not discriminate narrowband and broadband disturbance frequencies. As a result, the narrowband components at 50 Hz and 100 Hz are reduced merely by around 15 and 10 db, respectively.

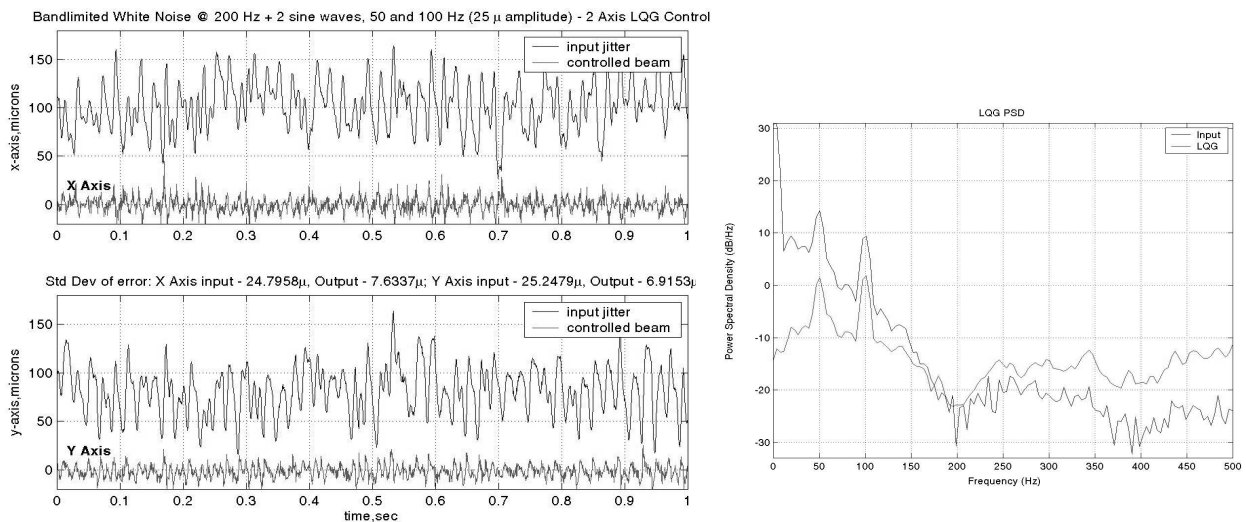


Figure 5. LQR Response

4.2. Wiener filter response

As a baseline for study of the adaptive filter, data taken from the experimentally induced jitter was filtered through the ideal Wiener filter offline, and the results presented in Figure 6. The power spectral density for the Wiener filter is also provided on each of the adaptive responses as a means of comparison. Only one axis is shown for the Wiener filter because the system behavior for both axes is almost identical for the LJC testbed. The Wiener filter indicates that the ideal adaptive filter should reduce the amplitude of the input jitter by 85 percent with about 25 db and 20 db decreases in the PSD of the two narrowband components, respectfully.

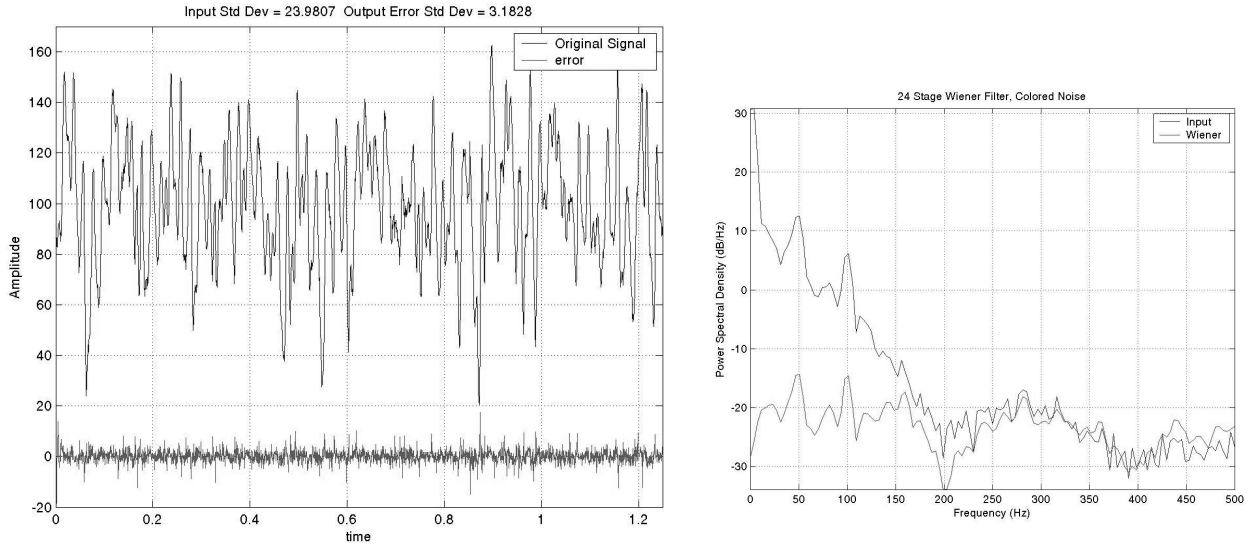


Figure 6. Wiener Filter Response

4.3. Adaptive LMS control response

The LMS controller was developed using the LMS adaptive filter from the Digital Signal Processing Toolbox of MATLAB. An adaptation rate of 0.1 was determined to be optimum for both axes by experimentation. A value of 1.0 for the leakage factor provided the best results. The LMS controller performed well for the colored noise disturbance, approaching the Wiener filter values. LMS control resulted in a greater than 80 percent decrease in the input jitter.

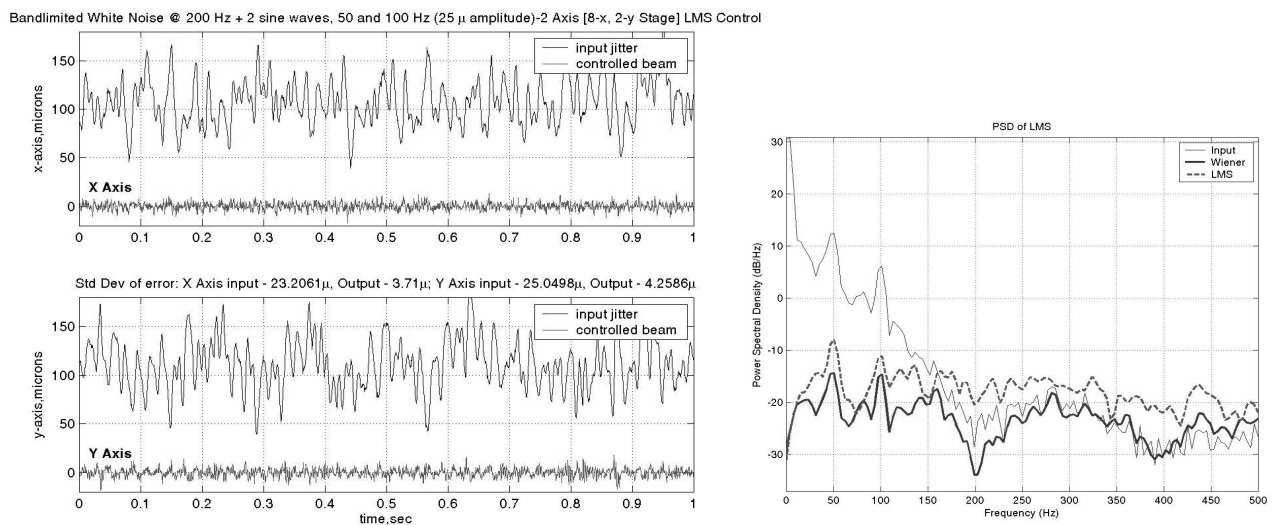


Figure 7. LMS response

4.4. GAL control response

The GAL algorithm was developed from that given in Table 12.1 of Ref. 6. The small, positive constants required by this algorithm, δ and a were set to 0.01. The “forgetting factor”, β , was set to 0.5, and μ , the adaptation rate, was 0.01. The algorithm was coded in C language into an “S-function” for use in the Real Time Workshop required for xPC Target³.

The GAL algorithm achieved about a 75 percent reduction in the input jitter, not too much better than the LQR controller. This may be due to approximate nature of the GAL algorithm as described in Ref. 6. A more stringent order-recursive lattice filter may provide better results and is the subject of further studies.

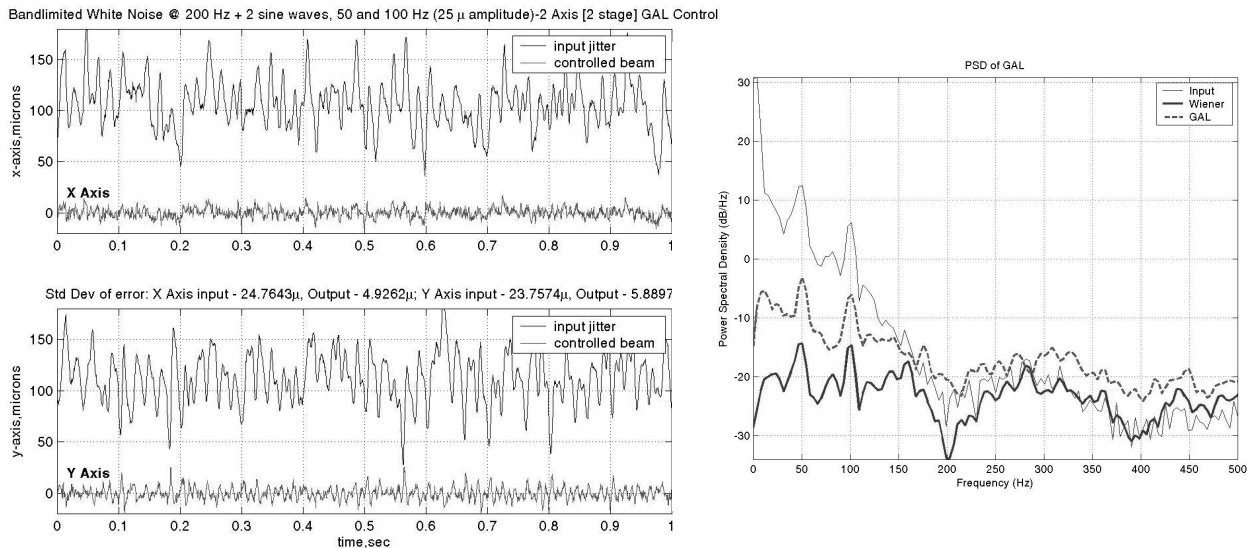


Figure 8. GAL response

4.5. GAL/LQG/LMS comparison

The results obtained in all previous sections are put together here for comparison. Figure 10 shows that both adaptive algorithms, LMS and GAL, achieve superior performance than that of the LQR method in suppressing the injected colored noise, with the LMS algorithm’s performance very close to that of the ideal Wiener filter. The standard deviation of both the effect of the input jitter and the response of all three controllers on each axis are summarized in Table 1.

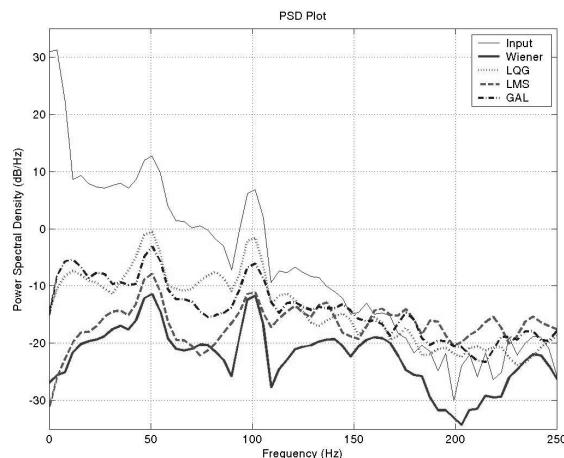


Figure 10. PSD of LQG, LMS, and GAL compared to the Wiener Filter

Table 1. Comparison of Controllers

Controller	LQR		LMS		GAL	
	X-axis	Y-axis	X-axis	Y-axis	X-axis	Y-axis
Input Jitter, Std. Dev, μm	24.8	25.2	23.2	25.0	24.8	23.8
Controlled Beam, Std Dev., μm	7.6	6.9	3.7	4.3	4.9	5.9
No. of stages/order	n/a	n/a	8	2	2	2
% reduction in jitter	69	73	84	83	80	75
db reduction in PSD of 50 Hz	-12	-12	-20	-20	-16	-16

4.6. Optimal stage number for adaptive algorithms

A series of experiments were conducted to determine the optimum filter order for the LMS filter and the optimum number of stages for the GAL filter. The percent reduction achieved in correcting the input jitter is plotted versus the number of stages (GAL) or order (LMS) of the adaptive filter. As is apparent from Figure 11, the LMS filter outperformed the GAL filter, regardless of the number of stages. The average execution time for each step was also documented to observe how efficient each algorithm was. In our current implementation, as can be seen from the graph, the execution time of the GAL algorithm rapidly approached the discrete sample time of 500 micro-seconds, and in fact the controller was unable to execute a 64 stage filter due to the execution time exceeding the sample time. The LMS algorithm stayed essentially constant as the order was increased. It is also interesting to note that as the execution time for the GAL algorithm increased, the ability to control the jitter decreased. This contradicts the general notion that the GAL algorithm, using lattice filters, yields a better computational efficiency than LMS algorithm, and therefore requires further study.

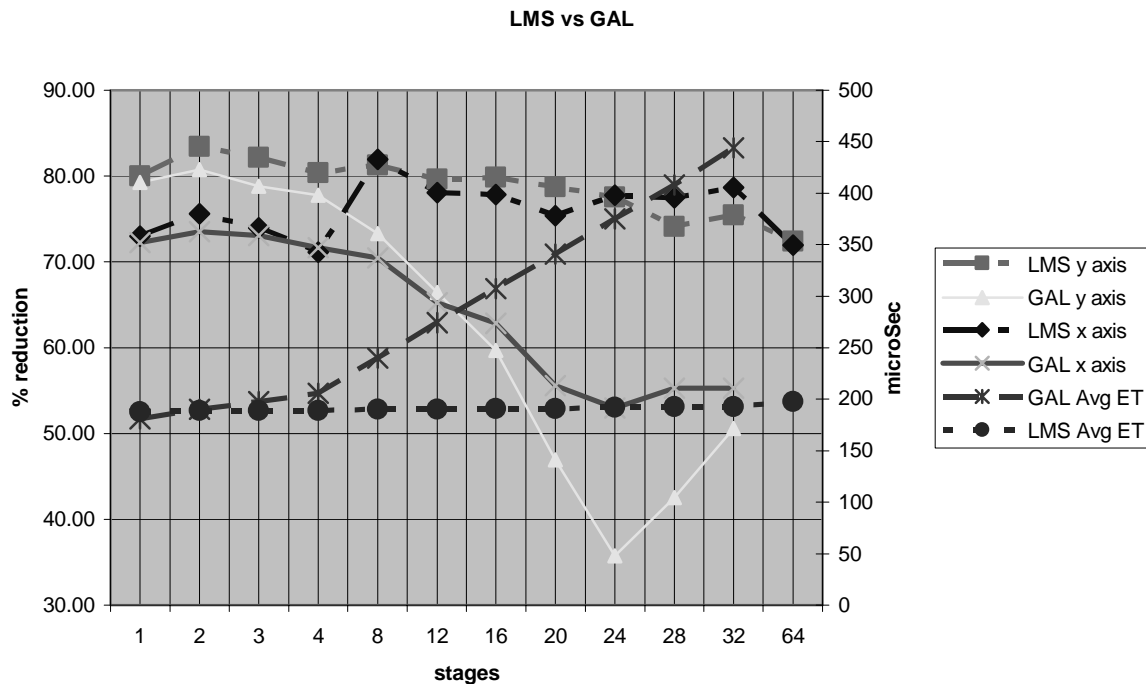


Figure 11. Percent reduction (in individual axis) and execution time (of each algorithm for both axes) vs. Number of Stages

5. CONCLUSION

A laser jitter control testbed has been constructed and three control algorithms have been tested on their effectiveness in suppressing the effect of injected colored noise. The initial experiments indicate that both adaptive LMS and GAL algorithms result in better jitter reduction than does the classical LQR control method, using a second order system model in determining the LQ-optimal gains. A better LQR controller would most certainly be obtained by using a more exact higher order model. However, the adaptive schemes, which do not rely on mathematical models, should still perform at least as well, if not better than the LQR. In our current implementation, GAL does not show the predicted advantage over the LMS: GAL's performance decreases and execution time increases rapidly with the stage number while those of the LMS stay about the same. All the control schemes investigated in this paper take the SISO approach in each axis of the control mirror. As the testbed is actively under enhancement, our investigation will shift toward using full MIMO type of control which can obtain enhanced performance by taking into account the cross-coupling between axes, which will be reported in our next paper. Additionally, the platform containing the control FSM will be shaken mechanically to induce vibrations in the control mirrors.

ACKNOWLEDGEMENT

The authors wish to acknowledge the help of Prof. Roberto Cristi for his insights into adaptive filter theory.

REFERENCE

1. Baker Adaptive Optics Homepage: <http://www.flash.net/~jtbaker/>
2. Newport Corp. Fast Steering Mirror webpage: <http://www.newport.com/semi/Products/Optics/product.asp?id=3881>
3. The Mathworks Inc., xPC Target webpage: <http://www.mathworks.com/products/xpctarget/>
4. On-Trak Photonics Inc., Position Sensing Modules webpage: <http://www.on-trak.com/psm.html>
5. B. Friedland, *Control System Design: An Introduction to State-Space Methods*, McGraw-Hill, New York, 1986
6. S. Haykin, *Adaptive Filter Theory*, Prentice-Hall, New Jersey, 2002
7. Widrow, B. and Stearns, S.D., *Adaptive Signal Processing*, Prentice-Hall, New Jersey, 1985
8. Edwards, S.G., "Active Narrowband Disturbance Rejection on an Ultra Quiet Platform", Dissertation, Naval Post Graduate School, Monterey, CA, 1999.
9. H. J. Chen, R. W. Longman, B. N. Agrawal, M. Q. Phan, S. G. Edwards, "Rejection of Multiple Unrelated Periodic Disturbances Using MELMS with Disturbance Identification," *Advances in the Astronautical Sciences*, Vol. 108 (Part I), 2001, Proceedings of the 11th AAS/AIAA Space Flight Mechanics Meeting, Feb 11-15 2001, Santa Barbara, CA, p 587-606.
10. Jiang S.-B. and Gibson, J.S., "An Unwindowed Multichannel Lattice Filter with Orthogonal Channels", *IEEE Transactions on Signal Processing*, Vol. 43, No. 12, pp 2831-2842, 1995
11. Chen, S.-J. and Gibson, J.S., "Feedforward Adaptive Noise Control with Multivariable Gradient Lattice Filters", *IEEE Transactions on Signal Processing*, Vol. 49, No. 3, pp 511-519, 2001